

— Supplementary Information —

**Adsorption Properties of Acetylene, Ethylene and Ethane  
in UiO-66 with Linker Defects and NO<sub>2</sub> Functionalization**

H. Pandey,<sup>1,2</sup> T. Barrett,<sup>2,3</sup> M. D. Gross,<sup>2,4</sup> and T. Thonhauser<sup>1,2</sup>

<sup>1</sup>*Department of Physics, Wake Forest University, Winston-Salem, NC 27109, USA.*

<sup>2</sup>*Center for Functional Materials, Wake Forest University, Winston-Salem, NC 27109, USA.*

<sup>3</sup>*Department of Chemistry, Wake Forest University, Winston-Salem, NC 27109, USA.*

<sup>4</sup>*Department of Engineering, Wake Forest University, Winston-Salem, NC 27109, USA.*

**I. ADDITIONAL FIGURES AND TABLES**

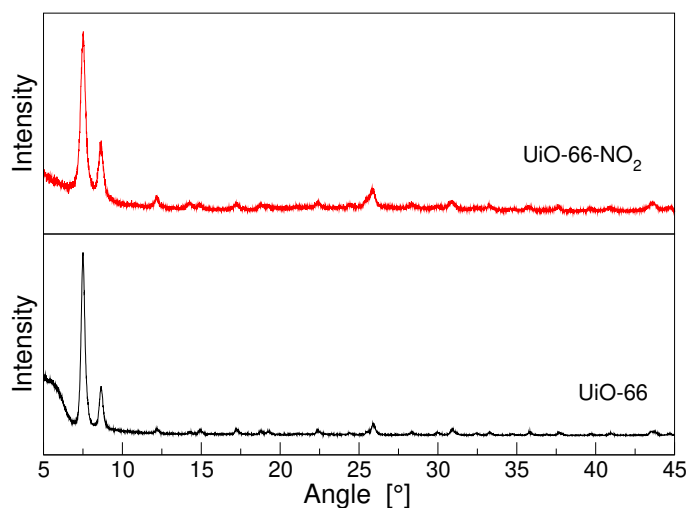


FIG. S1. Powder X-ray diffraction patterns were collected with a Bruker D2 Phaser X-ray diffractometer using CuK $\alpha$  radiation. The  $2\theta$  value range was 5° to 45°, the  $2\theta$  increment was 0.01°, the time step was 0.1 s, and the stage was rotated at 1 revolution per minute. The results confirm the formation of the crystalline UiO-66 phase as reported in the literature.<sup>1</sup>

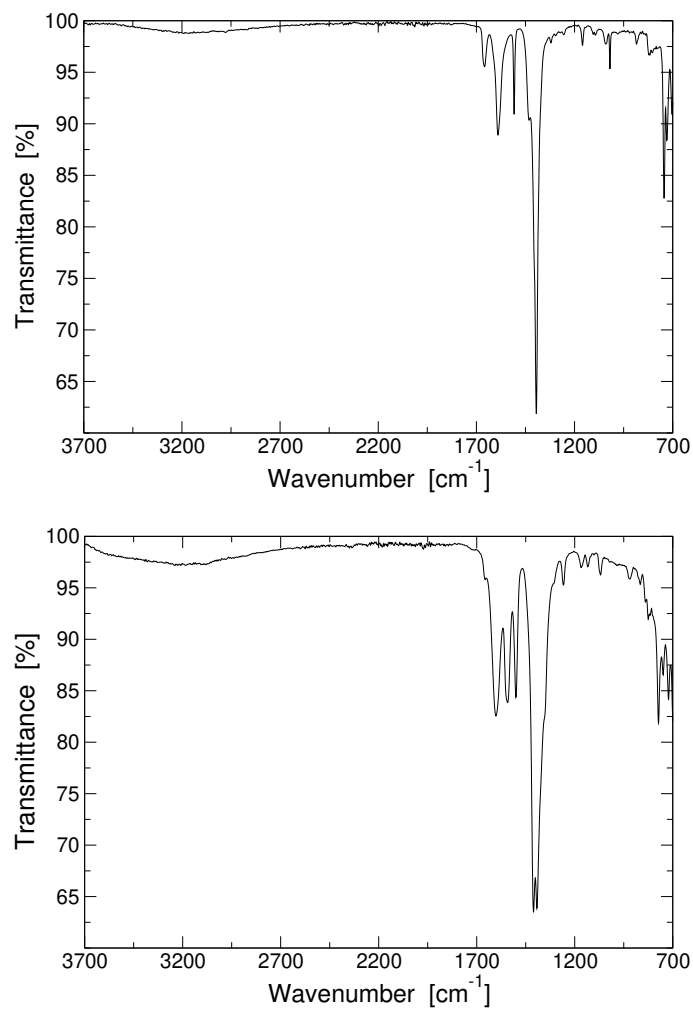


FIG. S2. A Perkin Elmer 100 FTIR spectrometer was used to probe the bond vibrations of UiO-66 and UiO-66-NO<sub>2</sub>. Powders of each sample were directly placed on the IR holder and pressed with a built-in press. The IR spectrum was acquired between 650 and 4000 cm<sup>-1</sup>. Both results match previously reported IR spectra<sup>1</sup> and confirm the presence of NO<sub>2</sub> in UiO-66-NO<sub>2</sub>.

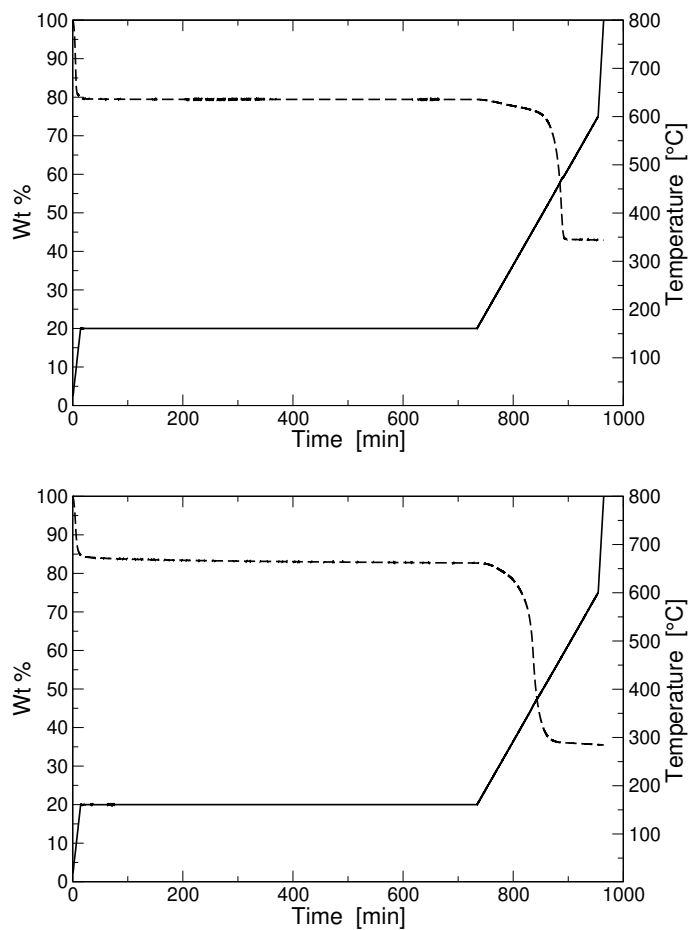


FIG. S3. Thermogravimetric analysis (SDT Q600, TA Instruments) was used to investigate the number of missing linker defects in UiO-66 and UiO-66-NO<sub>2</sub>. Samples were heated from ambient temperature to 160 °C at a ramp rate of 10 °C/min, held at 160 °C for 12 h, heated to 600 °C at a ramp rate of 2 °C/min, and then heated to 800 °C at a ramp rate of 10 °C/min. The hold at 160 °C was used to activate the sample prior to decomposition. The final weight was assumed to be ZrO<sub>2</sub>, which was confirmed by X-ray diffraction. The number of missing linker defects was calculated using the activated weight and final weight.

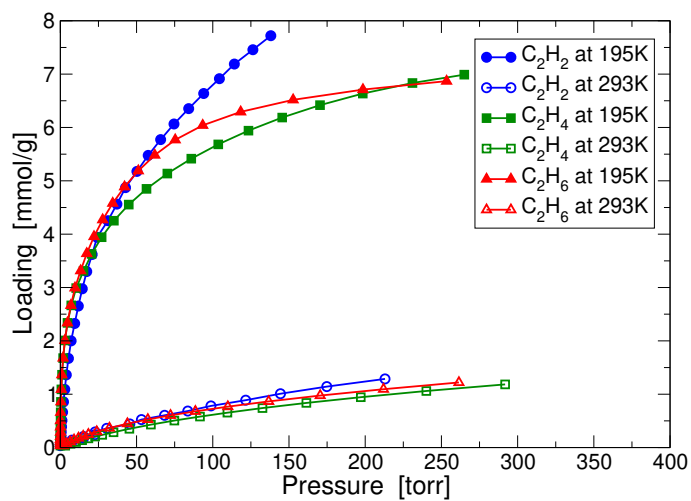
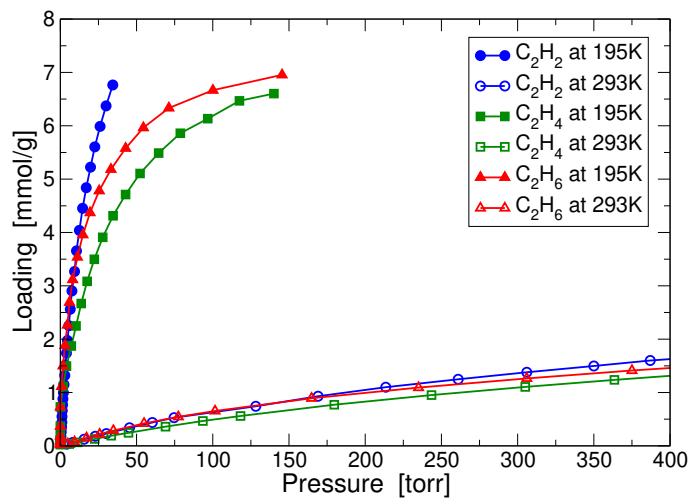


FIG. S4. C<sub>2</sub>H<sub>2</sub>, C<sub>2</sub>H<sub>4</sub> and C<sub>2</sub>H<sub>6</sub> isotherms for UiO-66 and UiO-66-NO<sub>2</sub> at 195 K and 293 K.

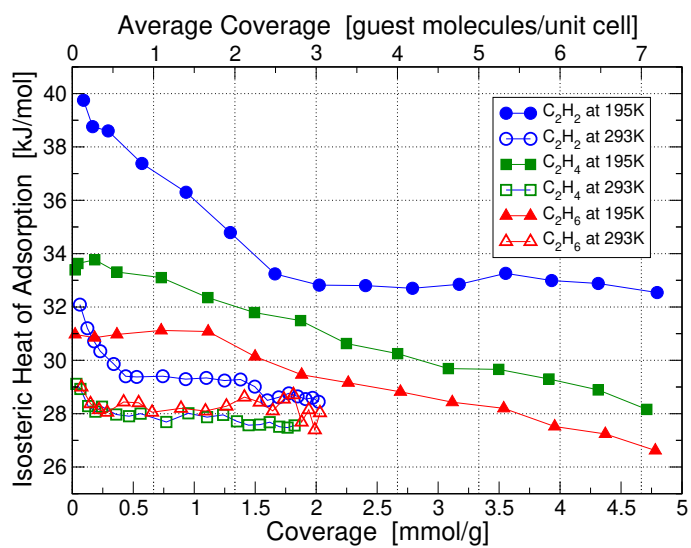


FIG. S5. Isosteric heats of adsorption of C<sub>2</sub>H<sub>2</sub>, C<sub>2</sub>H<sub>4</sub> and C<sub>2</sub>H<sub>6</sub> in UiO-66(Zr) at 195 K and 293 K, obtained by calorimetry measurements.

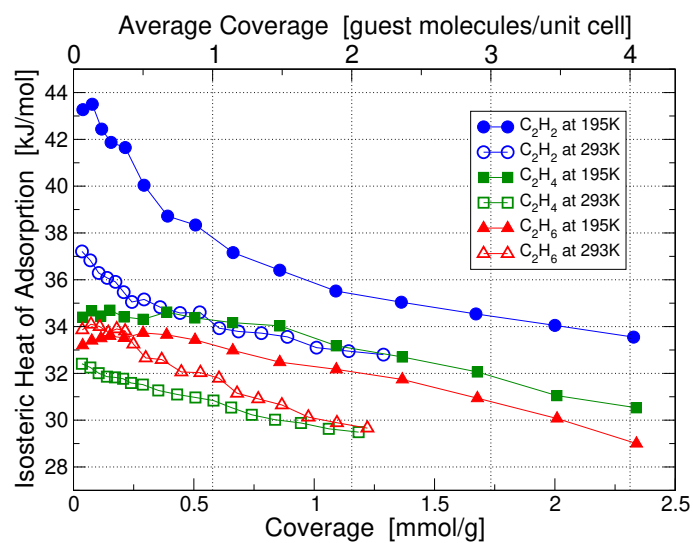


FIG. S6. Isosteric heats of adsorption of  $C_2H_2$ ,  $C_2H_4$  and  $C_2H_6$  in UiO-66(Zr)- $NO_2$  at 195 K and 293 K, obtained by calorimetry measurements.

TABLE S1. Experimentally determined average number of linkers per unit cell and BET specific surface area for UiO-66(Zr) and UiO-66(Zr)-NO<sub>2</sub>. Theoretical BET specific surface areas as a function of linkers per unit cell are shown for comparison.<sup>2</sup>

		linkers per unit cell	BET surface area (m <sup>2</sup> ·g <sup>-1</sup> )
UiO-66	experiment	4.61	1292
	theory	4	800
		6	1550
UiO-66-NO <sub>2</sub>	experiment	5.20	831
	theory	4	500
		6	1100

---

<sup>1</sup> M. Kandiah, M. H. Nilsen, S. Usseglio, S. Jakobsen, U. Olsbye, M. Tilset, C. Larabi, E. A. Quadrelli, F. Bonino, and K. P. Lillerud, *Chem. Mater.* **22**, 6632 (2010).

<sup>2</sup> M. J. Katz, Z. J. Brown, Y. J. Colón, P. W. Siu, K. A.

Scheidt, R. Q. Snurr, J. T. Hupp, and O. K. Farha, *Chem. Commun.* **49**, 9449 (2013).